Efficient, tunable, and coherent 0.18–5.27-THz source based on GaSe crystal

Wei Shi and Yujie J. Ding

Department of Electrical and Computer Engineering, Lehigh University, Bethlehem, Pennsylvania 18015

Nils Fernelius

Materials Directorate, Air Force Research Laboratory, AFRL/MLPS, Wright-Patterson Air Force Base, Ohio 45433

Konstantin Vodopyanov

Blue Leaf Networks, Suite H, 1050 East Duane Avenue, Sunnyvale, California 94085

Received April 16, 2002

Continuously tunable and coherent radiation in the wide range 56.8−1618 μm (0.18–5.27 THz) has been achieved as a novel and promising terahertz source based on collinear phase-matched difference frequency generation in a GaSe crystal. This source has the advantages of high coherence, simplicity for tuning, simple alignment, and stable output. The peak output power for the terahertz radiation reaches 69.4 W at a wavelength of 196 μm (1.53 THz), which corresponds to a photon conversion efficiency of 3.3%. A simple optimization of the design can yield a compact terahertz source.

OCIS codes: 190.2620, 140.3070, 140.4360, 190.4400.

Terahertz (THz) pulses generated by subpicosecond laser pulses based on photoconduction and optical rectification with a broad bandwidth have found many applications, such as THz imaging, THz spectroscopy for studies of carrier dynamics and intermolecular dynamics in liquids, and dielectric responses of molecules, polymers, and semiconductors.[1–8] A tunable and coherent THz source is one of the key elements for applications such as chemical identification, biomedical diagnostics, and THz spectroscopy.[8,9] For example, THz-probing technology exhibits a unique potential for label-free detection of a DNA binding state.[9] Furthermore, it was recently demonstrated that cw THz waves can be used to detect cancer. To achieve these important applications and therefore to create a new era for THz science and technology a compact, efficient, and coherent THz source is essential. However, so far the only such source that has wide tunability in the wavelength range 30−3000 μm has been costly free-electron lasers.[8] Ideally, new-generation THz sources should have the advantages of compactness, broad tunability, simple alignment, and stable THz output. cw THz radiation generated by optical-heterodyne (photo) mixing faces the unbreakable barrier of low output power (in the range of microwatts).[10,11] Another technique is based on nonlinear difference-frequency mixing in nonlinear optical (NLO) crystals.[12] For example, 4-dimethylamino-*N*-methyl-4-stilbazolium-tosylate (DAST) was recently used to generate coherent THz waves that are tunable from 120 to 160 μm but with the highest output energy of only 52 fJ/pulse (average power of 52 pW) through difference-frequency generation (DFG).[13] A THz optical parametric oscillator was recently investigated by use of $LiNbO_3$.[14] However, large absorption coefficients of $LiNbO_3$ and DAST in the THz domain result in low efficiencies and limited tunability.[13,14] Coherent THz emission based on intersubband transitions has not yet been implemented.[15–17]

In our recent study of coherent THz radiation we showed that, among the many NLO crystals such as $LiNbO_3$, $LiTaO_3$, $ZnGeP_2$, GaSe, DAST, CdSe, GaP, and GaAs, GaSe has the lowest absorption coefficients in the THz wavelength region.[18–20] Such a low absorption coefficient is extremely important for coherent THz generation because the overall conversion efficiency is limited by the effective absorption length. Furthermore, this material has a large birefringence. Consequently, phase matching can be achieved in an ultrabroad wavelength range. Even though GaSe has the potential to reach THz optical parametric oscillation (OPO) with a single pump beam,[19] DFG offers relative compactness, simplicity for tuning, straightforward alignment, much lower pump intensities, and stable THz output. Indeed, unlike OPO, DFG does not require a complicated alignment procedure, even if wavelength tuning is required. The high second-order NLO coefficient (d_{22} = 54 pm/V) and large figure of merit $d_{\mathrm{eff}}{}^2/n^3$ for GaSe make that compound the superior material for efficient THz generation. We can actually define a new figure of merit, $d_{\mathrm{eff}}{}^2/n^3\alpha^2$, in addition to the absorption coefficient in the THz wave. It turns out that the value of this figure of merit for GaSe is a factor of $\sim 9 \times 10^4$ larger than that of bulk $LiNbO_3$ at $\sim$200 μm.[18–20]

The experimental setup is shown in Fig. 1. As a DFG pump source we used a Nd:YAG laser (duration, 10 ns; pulse energy, 6 mJ; repetition rate, 10 Hz). As a second (tunable source) we used the output of a β-BaB_2O_4–based optical parametric oscillator pumped by the third harmonic of the same laser with the following parameters: duration, 5 ns; pulse energy, 3 mJ; repetition rate, 10 Hz. The peak intensity for the Nd:YAG pump beam was $\sim$17 MW/cm^2, which is below the optical damage threshold 30 MW/cm^2 of GaSe for similar pulse durations.[18] This pump intensity was $\sim$30 times lower than that used for achieving THz OPO in $LiNbO_3$.[14] The THz wave generated from the GaSe crystal was collimated

0146-9592/02/161454-03$15.00/0

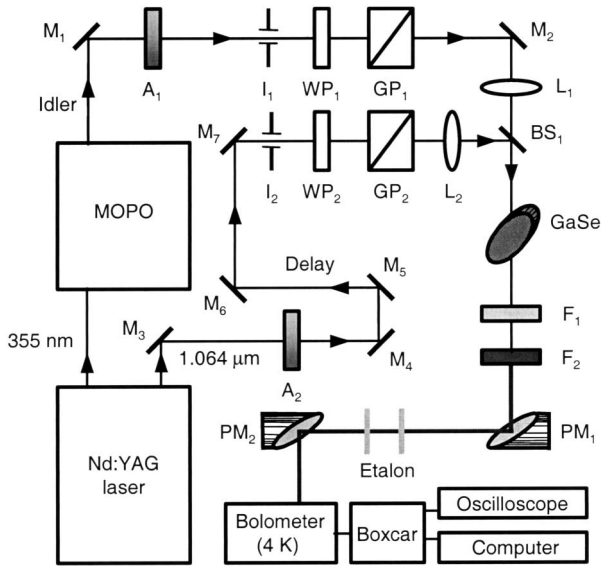

Fig. 1. Experimental setup for THz radiation based on DFG in a GaSe crystal: M_1–M_7, mirrors; A_1, A_2, attenuators; I_1, I_2, irises; WP_1, WP_2, $\lambda/2$ plates; GP_1, GP_2, Glan polarizers; BS_1, 50/50 beam splitter, L_1, L_2, convex lenses with $f = 10$ and $f = 20$ cm, respectively; PM_1, PM_2, parabolic mirrors; F_1, F_2, germanium and black polyethylene filters, respectively. MOPO, master oscillator power oscillator. The etalon is made from two parallel germanium plates mounted upon two mirror mounts on two separate translation stages.

and then focused into a Si bolometer by two off-axis parabolic metal mirrors. We first used a 15-mm-long z-cut GaSe crystal with a 35 mm × 20 mm elliptical aperture and no antireflection coatings. For type-*oee* phase-matching (PM) interaction (o and e indicate ordinary and extraordinary polarization, respectively, of the beams inside the GaSe crystal), the effective NLO coefficients for GaSe depend on the PM (θ) and azimuthal (φ) angles as $d_{\text{eff}} = d_{22} \cos^2 \theta \cos 3\varphi$.[18] To optimize d_{eff}, azimuthal angles of $\varphi = 0°$, $+60°$, $+120°$, $\pm 180°$ can be chosen such that $|\cos 3\varphi| = 1$, as was confirmed in our experiment.

Figure 2 shows the external PM angular tuning curves for the type-*oee* collinear DFG THz radiation. We observed the phase-matching peaks by varying θ and one of the pump wavelengths (circles in Fig. 2). Tunable and coherent THz output radiation in the extremely wide range 56.8–1618 μm (0.18–5.27 THz) was achieved; see the inset of Fig. 2. The short-wavelength cutoff for the THz output is due to the presence of the narrow lattice absorption band for GaSe, which peaks at 40 μm.[21] The long-wavelength end, however, is limited by the measurable THz signal because it decreases as the output wavelength increases.[22]

Figure 3 shows the dependence of the THz wavelength on the OPO idler wavelength. Based on Figs. 2 and 3, the theoretical (based on Ref. 23) and experimental PM curves are in an excellent agreement over the entire range of the output wavelengths. The wavelength of the monochromatic THz wave was easily verified by use of a scanning etalon made from two Ge wafers (a finesse of ~4) shown in Fig. 1. Each of the measured THz wavelengths was consistent with that determined from the wavelengths of two incident pump beams used for DFG.

This THz radiation had a pulse duration of 5 ns and a repetition rate of 10 Hz. The measured THz peak output powers for the 15-mm-thick GaSe crystal at different THz output wavelengths are shown in Fig. 4. We also plotted the measured THz peak output powers versus the output wavelength for two other GaSe crystals with lengths of 4 mm and 7 mm. The three GaSe crystals have different THz tuning ranges: 56.8–810 μm for 4 mm, 56.8–944 μm for 7 min, and 56.8–1618 μm for 15 mm. They also have different maximum THz peak output powers with different corresponding peak wavelengths: 4 mm, 10.5 W at 106 μm; 7 mm, 17.0 W at 146 μm; and

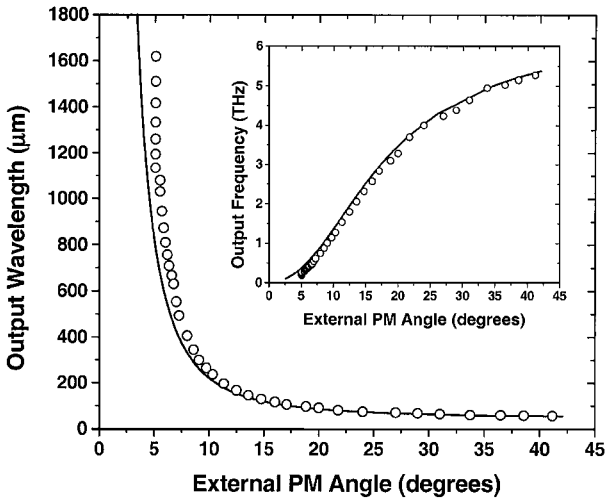

Fig. 2. Output wavelength versus external PM angle. Inset, output frequency versus external PM angle. Circles and solid curves, respectively, correspond to experimental and calculated results of refractive-index dispersion relations for GaSe in Ref. 23.

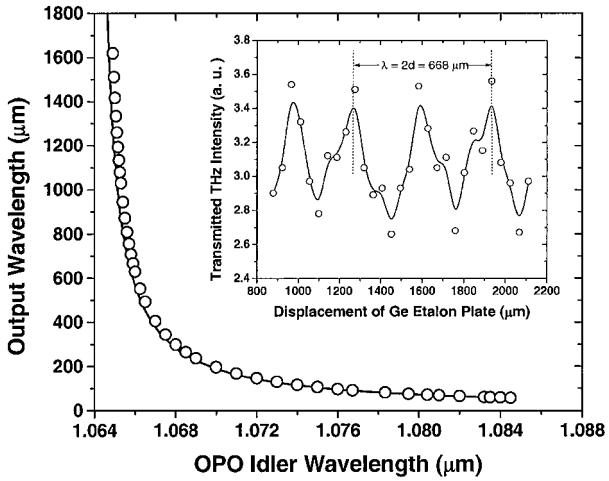

Fig. 3. Ouptut wavelength versus OPO idler wavelength based on DFG. Circles and solid curve correspond to experimental and calculated results, respectively, by use of the photon-energy conservation relation. Inset, measurement of THz wavelength (668 μm) by a scanning Ge etalon. Circles, experimental results; solid curve, B-splined result from data.

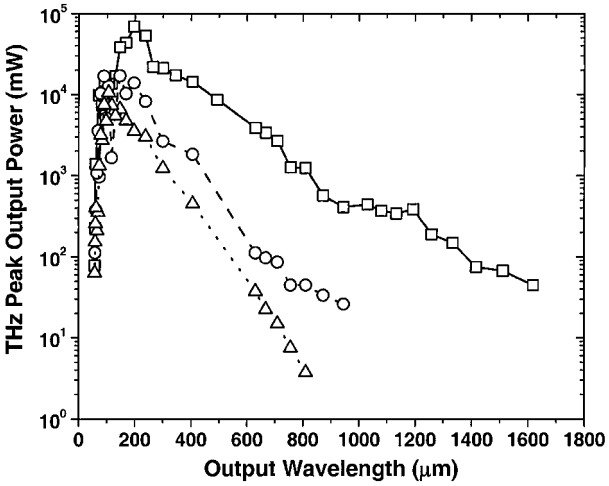

Fig. 4. Peak output power versus output wavelength for three pure GaSe crystals with thicknesses (along the z axis) of 4 mm (triangles), 7 mm (circles), and 15 mm (squares).

15 mm, 69.4 W at 196 μm. Three maximum THz peak output powers correspond to conversion efficiencies of 1.77×10^{-5}, 4.5×10^{-5}, and 1.8×10^{-4}, with corresponding photon conversion efficiencies of 0.18%, 0.62%, and 3.3%. Obviously the highest THz peak output powers are determined by the effective absorption lengths of the GaSe crsytal in the THz domain, which are larger than 15 mm. The power conversion efficiency can be calculated from Ref. 22:

$$\frac{P_1}{P_2} = \frac{1}{2}\left(\frac{\mu_0}{\epsilon_0}\right)^{3/2}\frac{\omega_1{}^2 d_{\mathrm{eff}}{}^2 L^2}{n_1 n_2 n_3}\left(\frac{P_3}{\pi w^2}\right)T_1 T_2 T_3 \times \exp(-\alpha_1 L)\left[\frac{1-\exp(-\Delta\alpha L/2)}{\Delta\alpha L/2}\right]^2,$$

where $T_j = 4n_j/(n_j + 1)^2$ is the Fresnel transmission coefficient for each facet and the subscripts $j = 1, 2, 3$ correspond to the THz wave and the two pump waves, respectively, $\Delta\alpha = |\alpha_2 + \alpha_3 - \alpha_1|$, and w is the beam size for the pump. Typically, w is measured to be $\sim$1 mm. The theoretical conversion efficiencies, which correspond to the three maximum output powers cited above, are calculated to be 3.1×10^{-5}, 9.6×10^{-5}, and 4.4×10^{-4}, respectively.

In conclusion, an efficient and coherent THz source that is tunable in the extremely wide range 56.8–1618 μm has been achieved. The maximum peak output power reached 69.4 W at 196 μm, with a pulse width of $\sim$5 ns. These tuning ranges and peak powers are much superior to those obtained previously by DFG.[12,13] Compared with THz generation based on OPO, highly efficient THz waves can be generated from a GaSe crystal by use of much lower pump intensities.[14] Moreover, the DFG output wavelengths and powers are much more stable than those based on OPO. Our result has laid a solid foundation for what is to our knowledge the first commercial THz source that is tunable in the broad frequency domain. We have demonstrated that GaSe is indeed the best nonlinear optical material used for THz generation in terms of absorption coefficient in the THz domain and of the nonlinear coefficient. Following our result, it is feasible to achieve cw emission by use of DFG in GaSe, although one should use pump wavelengths much longer than 1 μm to avoid two-photon absorption.

W. Shi and Y. J. Ding are adjunct members of the University of Arkansas. The authors are indebted to V. G. Voevodin, who grew the GaSe crystals used in this research. This research was supported by the U.S. Air Force Office of Scientific Research and the National Science Foundation. Y. J. Ding's e-mail address is yud2@lehigh.edu.

References

1. B. B. Hu and M. C. Nuss, Opt. Lett. **20,** 1716 (1995).
2. Q. Chen, Z. Jiang, G. X. Xu, and X.-C. Zhang, Opt. Lett. **25,** 1122 (2000).
3. J. L. Johnson, T. D. Dorney, and D. M. Mittleman, Appl. Phys. Lett. **78,** 835 (2001).
4. M. Schall and P. U. Jepsen, Opt. Lett. **25,** 13 (2000).
5. C. Rønne, P. Åstrand, and S. R. Keiding, Phys. Rev. Lett. **82,** 2888 (1999).
6. T. I. Jeon, D. Grischkowsky, A. K. Mukherjee, and R. Menon, Appl. Phys. Lett. **77,** 2452 (2000).
7. Y. S. Lee, R. Meade, T. B. Norris, and A. Galvanauskas, Appl. Phys. Lett. **78,** 3583 (2001).
8. P. G. O'Shea and H. P. Freund, Science **292,** 1853 (2001).
9. M. Nagel, P. H. Bolivar, M. Brucherseifer, H. Kurz, A. Bosserhoff, and R. Büttner, Appl. Phys. Lett. **80,** 154 (2002).
10. E. R. Brown, F. W. Smish, and K. A. McIntosh, J. Appl. Phys. **73,** 1480 (1993).
11. S. Matsuura, G. A. Blake, R. A. Wyss, J. C. Pearson, C. Kadow, A. W. Jackson, and A. C. Gossard, Appl. Phys. Lett. **74,** 2872 (1999).
12. F. Zernike, Jr., and P. R. Berman, Phys. Rev. Lett. **15,** 999 (1965).
13. K. Kawase, T. Hatanaka, H. Takahashi, K. Nakamura, T. Taniuchi, and H. Ito, Opt. Lett. **25,** 1714 (2000).
14. K. Imai, K. Kawase, J.-I. Shikata, H. Minamide, and H. Ito, Appl. Phys. Lett. **78,** 1026 (2001).
15. L. Friedman, G. Sun, and R. A. Soref, Appl. Phys. Lett. **78,** 401 (2001).
16. R. Kohler, A. Tredicucci, F. Beltram, H. E. Beere, E. H. Linfield, A. G. Davies, and D. A. Ritchie, Appl. Phys. Lett. **80,** 1867 (2002).
17. I. Vurgaftman and J. R. Meyer, Appl. Phys. Lett. **75,** 899 (1999).
18. V. G. Dmitriev, G. G. Gurzadyan, and D. N. Nikogosyan, *Handbook of Nonlinear Crystals* (Springer-Verlag, Berlin, 1999), pp. 119–125, 166–169.
19. Y. J. Ding and I. B. Zotova, Opt. Quantum Electron. **32,** 531 (2000).
20. Y. J. Ding and J. B. Khurgin, Opt. Commun. **148,** 105 (1998).
21. E. D. Palik, *Handbook of Optical Constants of Solids* (Academic, New York, 1998), Vol. III.
22. A. Yariv, *Quantum Electronics* (Wiley, New York, 1988), p. 401.
23. K. L. Vodopyanov and L. A. Kulevskii, Opt. Commun. **118,** 375 (1995).